

# Strategies for the Optimal Classification of Volcanic Ash Granulometry

B. Andò, S. Baglio, V. Marletta

Dipartimento di Ingegneria Elettrica Elettronica e Informatica (DIEEI)

University of Catania

Catania, Italy

bruno.ando@dieei.unict.it

**Abstract**— The ash fall-out following explosion activity of volcanoes like the Mount Etna, represents a serious hazard for the safety of air traffic, causing, in many cases, flight cancellations or temporary closures of the airport with consequently inconvenience for passengers and loss of profit for airlines. Researchers at DIEEI of the University of Catania, in the framework of the SECESTA project have developed a low-cost smart multisensor system for the monitoring of ash fall-out phenomenon by measuring ash presence, average granulometry and ash flow-rate. The node, is intended to be integrated into a sensor network which will provide a distributed information useful to predict the time-space evolution and oriented to the implementation of an early warning approach for the monitoring of the phenomenon. This paper is particularly focused on the methodologies to be adopted for the choice of the optimal granulometry classification thresholds by using the ROC curves theory. Experimental investigations have been performed using ash erupted by Etna volcano.

**Keywords**— volcanic ash; ash fall-out; ash granulometry; granulometry classification; multisensors architecture; ROC curves.

## I. INTRODUCTION

It is well known the worldwide increasing in the volcanic activity with atmospheric dispersion of volcanic ash (coarse ash) and volcanic dust (fine ash). Both these two different grain size ashes represent a relevant factor of risk for human health and the safety of the air traffic. They can compromise the safety of the air transportation on different levels with different effects on aircraft components: because volcanic ash/dust particles are principally composed of silica they generally melt as they travel through the combustor stage and tend to solidify and deposit as they penetrate the 'cold' turbine section thus producing engine shutdown due to the clogging of the nozzle guide vanes of the jet engine; engine overheating (due to the accumulation of volcanic particles in the cooling system); erosion (due to their high abrasiveness) of both engine's parts and external components like windshield, body, wings, tailfin and empennage; alteration of the transmission's components (as finest particles may penetrate the sealing of the transmission system and get transported into the gear meshes); denting of the protective ceramic coatings of the turbine blades. Moreover, pneumatic controls and on-board instruments are also subject to clogging: for instance, the Pitot-static probes

which provide pilots with reliable air speed indications may be damaged [1]. Another aspect of the consequences of the volcanic activity is the operational disruption and physical damage at airports. The number of airports impacted by volcanic activity annually has an increasing trend [2]. The main threat to airports is ash fall-out, which can cause loss of visibility for safe landing and takeoff, create slippery runways, infiltrate communication and electrical systems, interrupt ground services, and damage buildings and parked airplanes [2]. In many cases the effect of the ash fall-out is the flight cancellations or temporary closures of the airport for hours to weeks with consequently inconvenience for passengers and loss of profit for airlines. This is the case of the Fontanarossa international airport in the South of Italy, which in last years has been repeatedly declared inappropriate for take-offs and landings because of ash plumes spewed by the Etna volcano.

A series of counteractions can be implemented in order to mitigate the effect of the volcanic ash such as covering parked aircraft, conducting clean-up quickly and efficiently to reduce closure time and modifying approach and take-off routes to avoid ash in nearby airspace [2]. However, it has been observed that in order to be effective, these mitigation efforts require an airport-specific operational plan describing methods and available equipment for clean-up, protocols for making the decision to close an airport to ensure aircraft and passenger safety, and procedures for managing air traffic in ash-contaminated airspace in the vicinity of the airspace. The Fontanarossa international airport is one of the airports known to have formulated some type of operational plan. Moreover the effectiveness is improved when airports have procedures for incorporating up-to-date information (received forewarning of imminent volcanic hazards) from the volcanology agency into operational decisions. In the specific case of the Fontanarossa airport, the National Institute of Geophysics and Volcanology (Istituto Nazionale di Geofisica e Vulcanologia, INGV) was designated as the primary source of information about eruptions that produce volcanic clouds. INGV is equipped with systems for monitoring ash clouds and forecasting their space-time evolution [3] to provide decision support for aeronautical authorities in order to significantly reduce the factors of unpredictability, and therefore the impact of the ash fall-out on airport infrastructure and flight operations.

Different techniques have been actually used worldwide to alert airports of volcanic activity. Real-time monitoring of explosive volcanoes by seismic and infrasonic instruments [2, 4], forecasts of ash dispersion and deposition [3, 5] and detection of approaching ash clouds using high cost instrumentation typically based on satellites [6], X-Band dual-polarization radars [7], ground Thermal InfraRed camera (TIR) [8] or ground-based Doppler radar [9] are some examples of adopted solutions. Although these solutions provide accurate information about the volcanic activity and ash fall-out phenomenon, they are expensive, difficult to be installed and maintained and are often used to perform spot measurements. Moreover, to provide a reliable support for aeronautical authorities, the forecasting models used to predict the time-space evolution of the ash fall-out phenomenon, should be supplied by spatially distributed information about characteristic parameters of the ash fall-out such as ash granulometry and flow-rate in addition to weather conditions. In this framework a distributed Wireless Sensor Network (WSN) of low cost monitoring stations would represent a suitable solution in performing a continuous monitoring of the phenomenon and gaining a high spatial resolution awareness of the ash fall-out.

The SECESTA project [10] aims at the development of an early-warning wireless network of low cost multisensor nodes for the measurement of typical parameters of volcanic ash fall-out phenomenon (flow-rate and granulometry) which will provide a spatially distributed information useful to predict the time-space evolution of ash fall-out [11-14]. Such forecast is useful to implement an optimal planning of actions required to both restore the airport functionalities and manage air traffic during the ongoing phenomenon. Although the early-warning network will provide a rough, less accurate information with respect to high cost instrumentation, it will enable experts to gain a time continuous awareness of the ash fall-out phenomenon with a high degree of spatial resolution. SECESTA is the Italian acronym for “A sensor network for the monitoring of volcanic ash fall-out for the safety of air transport”. The project is funded under the POR FESR Sicily 2007–2013 program and it exploits the synergic cooperation between research institutes (among which the DIEEI of Catania) and small-medium sized enterprises in charge of developing the final engineered version of the multisensor node and the WSN with the collaboration of the INGV, Catania Section. The WSN will monitor the ash fall-out phenomenon along the area spreading from main craters of the Etna volcano to the Fontanarossa international airport. Fig. 1 shows the monitored area and the topology of the WSN. Circles in Fig. 1 represent the multisensor nodes in the identified locations where they will be placed.

Researchers at DIEEI in Catania have developed a lab scale low cost prototype of the multi-sensor node to measure main quantities of interest for the considered phenomenon such as the ash flow-rate and the ash granulometry, by exploiting a self-powered  $\mu$ -controller based architecture. The developed methodologies for the discrimination of the volcanic ash from other types of sediments, ash granulometry detection and ash flow-rate estimation have been deeply discussed in [11-14] and supported by experimental results.

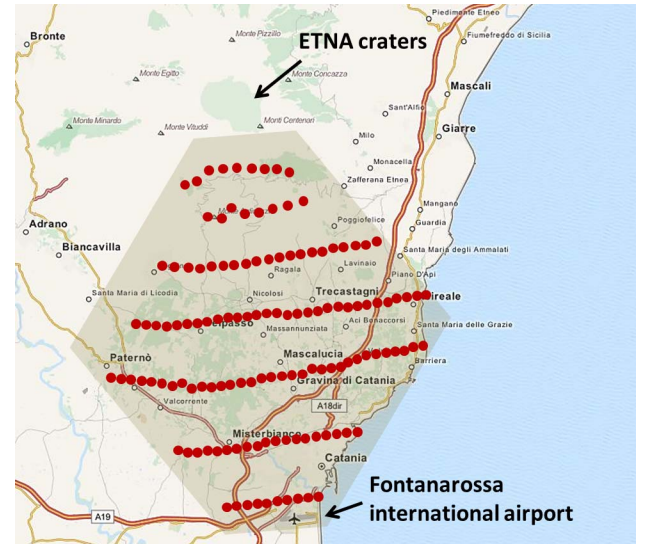


Fig. 1. The monitored area and the wireless network of multisensor nodes.

In particular [12] focused on the sensing methodology adopted for ash granulometry detection and experimental results obtained by the lab scale prototype with volcanic ash from Etna mount with three different granulometries (0.4 mm, 1 mm, 2 mm). Moreover, authors proposed Receiver Operating Characteristic (ROC) analysis as a theoretical support to properly implement the threshold mechanism aimed at ash granulometry classification just providing preliminary criteria to properly choose classification thresholds.

With respect to [12], in this paper three analytical methodologies to choose the optimal granulometry classification thresholds by using the ROC curves theory are discussed. Furthermore, new experimental results obtained with a new engineered implementation of the sensor for the granulometry detection and volcanic ash with three different granulometries (0.25 mm, 1 mm and 8 mm) are presented.

In the next section an overview of a new engineered version of the multisensor node is given. A description of the sensing strategy developed for ash granulometry estimation is provided in Section III for the sake of completeness. New experimental results will be presented in Section IV while the methodologies to choose the classification thresholds by using the ROC curves theory will be discussed in Section V.

## II. THE MULTISENSOR NODE

A schematization of the new engineered multisensor node with the on-board electronics is shown in Fig. 2. The system consists of a stainless steel funnel-shaped structure to convey the falling volcanic ash to an instrumented tank where a dedicated array of 40 (1 mm spaced), coupled InfraRed (IR) diodes-phototransistors allows for an indirect estimation of the volcanic ash flow-rate by monitoring the level of ash in the tank. By measuring the time required by the ash to fill the volume between two consecutive couple of IR detectors it is possible to estimate the flow-rate of the falling ash [14]. To provide the system with the required selectivity as respect to exogenous sediments like sand and water, a magnetic sensing strategy exploiting the paramagnetic behavior of the basaltic

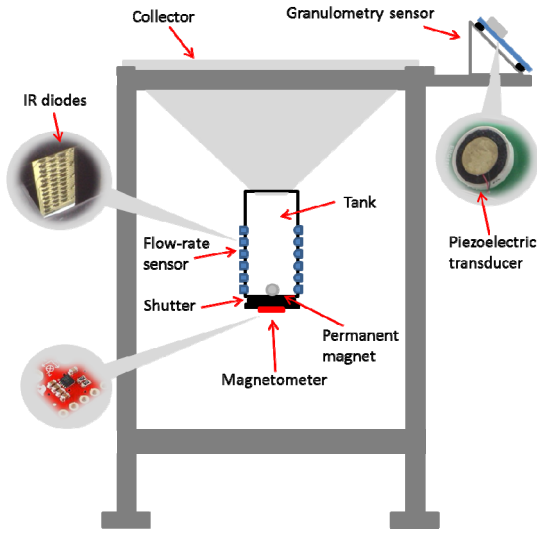


Fig. 2. Schematization of the multisensor node.

volcanic particles has been implemented [13-15]. To this purpose a low power digital magnetometer MAG3110 by Freescale Semiconductor has been used together with a permanent magnet to produce a biasing magnetic field. The volcanic ash particles in the tank will perturb the magnetic field produced by the permanent magnet, thus producing a variation of the magnetic sensor output. The sensor, communicates with the  $\mu$ -controller architecture by a digital I2C protocol. With respect to [13-14], in the new multisensor node the magnetic field sensor has been placed at the bottom of the tank. Moreover, to perform tank empty operations, a suitable shutter system has been designed.

The sensor for the granulometry detection exploits a piezoelectric transducer to convert the impacts of ash grains into electrical signals [11, 12].

Signals provided by sensors are acquired and processed by a  $\mu$ -controller architecture. Data are then transferred by a wireless transmission protocol (IEEE 802.15.4) to a dedicated PC station for the sake of debugging during the development phase of the system. To manage the multisensor node, test the correct operation and display the information from the sensors during the debugging phase, a on purpose LabVIEW VI has been developed. The Graphic User Interface (GUI) of the application is shown in Fig. 3.

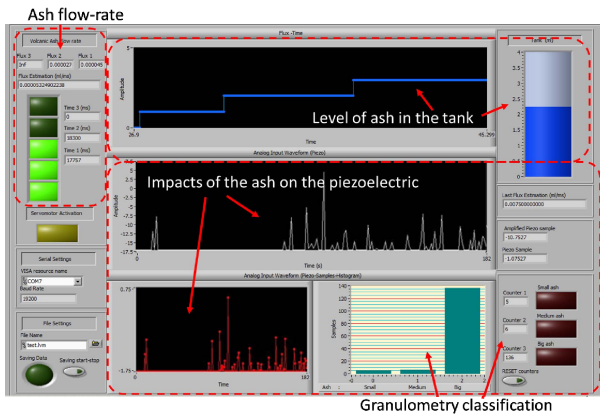


Fig. 3. GUI of the LabVIEW VI developed to manage the multisensor node.

### III. THE ASH GRANULOMETRY SENSOR

For the sake of completeness in this section a brief description of the methodology developed for the sake of granulometry detection is given.

The main idea underpinning the proposed methodology for ash granulometry classification is to exploit a piezoelectric transducer to convert ash impacts into electrical signals whose properties are strictly dependent on ash granulometry. The physical force provided by the impact of the ash grain on the transducer depends, in fact, on the particle granulometry [12]. As a consequence of the impact of the ash grain, the piezoelectric transducer oscillates at its characteristic natural frequency  $f_n$  following a typical decreasing exponential envelope as predicted by the following model:

$$V_{out} = g_{33} \frac{d}{S} K R_A^2 \frac{e^{-\xi \omega_n t}}{\sqrt{1 - \xi^2}} \sin(2\pi f_n t) \quad (1)$$

where  $\xi$  is the system damping,  $f_n$  is the natural frequency,  $g_{33} = 22 \text{e-}3 \text{ Vm/N}$  is the piezoelectric coefficient in the stress direction,  $d = 0.23 \text{e-}3 \text{ m}$  and  $S = 4.155 \text{e-}4 \text{ m}^2$  are the thickness and the surface area of the transducer, respectively, while  $R_A$  represents the radius of the ash particle under the hypothesis of modelling the ash grain as a linear elastic solid sphere [12]. Finally,  $K$  is a constant term given by:

$$K = 1.2644 \rho_A^{3/5} \left( \frac{1}{k_p + k_A} \right)^{2/5} v_A^{6/5} \quad (2)$$

where  $\rho_A = 2 \text{ kg/m}^3$ ,  $k_A$  and  $v_A$  represent the density, the stiffness and the terminal settling velocity [16] of the ash particle, respectively, and  $k_p$  represents the stiffness of the piezoelectric transducer.

As stated by Eq. (1) and already demonstrated in [12] the amplitude of the sensor's response is strictly related to the particle mass (impact force) or to its size (for a known particle density). As can be observed, the signal peak value increases with ash particle size.

It is important to note that the ash density (which fixes the relationship between granulometry and the mass of each particle) is an intrinsic characteristic of the volcano, and it can be considered as a known quantity. With respect to other sensing methodologies (e.g. capacitive or inductive), the proposed sensing strategy provides an information related to each particle bumping into the piezoelectric device. It avoids an indirect estimation of the average particle size, e.g. obtained by measuring the volume of collected ash.

With respect to the solution discussed in [12], a new implementation has been realized by placing the piezoelectric transducer (7BB-35-3L0 by Murata) on a FR4 sheet fixed on a stainless steel support. The piezoelectric transducer is placed with a slope of  $45^\circ$  with respect to the vertical axis with the aim to reduce multiple impacts of the same ash grain due to undesired bounces. A rain sensor has been realized on the same FR4 sheet. The piezoelectric transducer has been mechanically insulated from the support structure by a suitable dumper in order to reduce the effect of vibrations due to the ash grains impacting on the support.

#### IV. EXPERIMENTAL RESULTS

A new set of experiments has been performed with the new granulometry sensor employing volcanic ash from the mount Etna. Results presented in this paper have been obtained by using three classes of particle with an average radius of around 0.25 mm, 1 mm and 8 mm.

Fig. 5 shows the typical piezoelectric response to a single ash particle impact for the three ash granulometries considered in this paper. A peak due to a second ash grain is also visible in Fig. 5c. As can be observed, the signal peak value increases with ash particle size.

Distributions of observed voltage peak amplitudes, at the output of the conditioning electronics of the piezoelectric transducer, for the three granulometries investigated are shown in Fig. 6. As can be observed, distributions partially overlap. Anyway, the average values of the considered output quantity (the voltage peak), are well separated [12]. Moreover, as expected, the distribution between the large granulometry (8 mm) and the small granulometry (0.25 mm) are separated [12].

On the basis of such considerations, the ash granulometry classification problem can then be faced as two separated binary classification problems. The Receiver Operating Characteristic (ROC) curves theory provides an analytical method for the evaluation of the performance of the classifier as the discrimination threshold is varied [17]. Applying the theory of ROC curves to the ash granulometry problem, taking into account the distribution of voltage peaks in Fig. 6, curves in Fig. 7a and 7b have been obtained for the two classification problems between 0.25 mm sized ash grains and 1 mm sized grains and between 1 mm sized grains and 8 mm sized grains, respectively.

Considering that each point on the ROC curve identifies a threshold value, the following step consists of fixing suitable thresholds for the two classification problems. As emerges from Fig. 7 and consistently with information in Fig. 6, suitable thresholds values, T1 and T2, discriminating 0.25 mm sized grains from 1 mm grains and grains of 1 mm sized grains from 8 mm grains, with very good performances, can be easily defined.

Although the operative context (position of the monitoring station and weather conditions) should be taken into account, some preliminary criteria to properly choose classification thresholds was drawn in [12] by taking into account the need for a correct classification of smaller size particles which can be transported over longer distances. In the next Section three analytical methodologies to choose the optimal granulometry classification thresholds by using the ROC curves theory are discussed.

#### V. STRATEGIES FOR THE OPTIMAL THRESHOLD SELECTION

The choice of the threshold represents a tricky phase in the classification problems. The performance of the classifier is strictly related to the chosen threshold value. A first possible approach could be to find a threshold value providing a good compromise between the Sensitivity and the Specificity of the classifier [12]. As an example, a possible solution could be the value of the threshold which makes equals the two indexes as

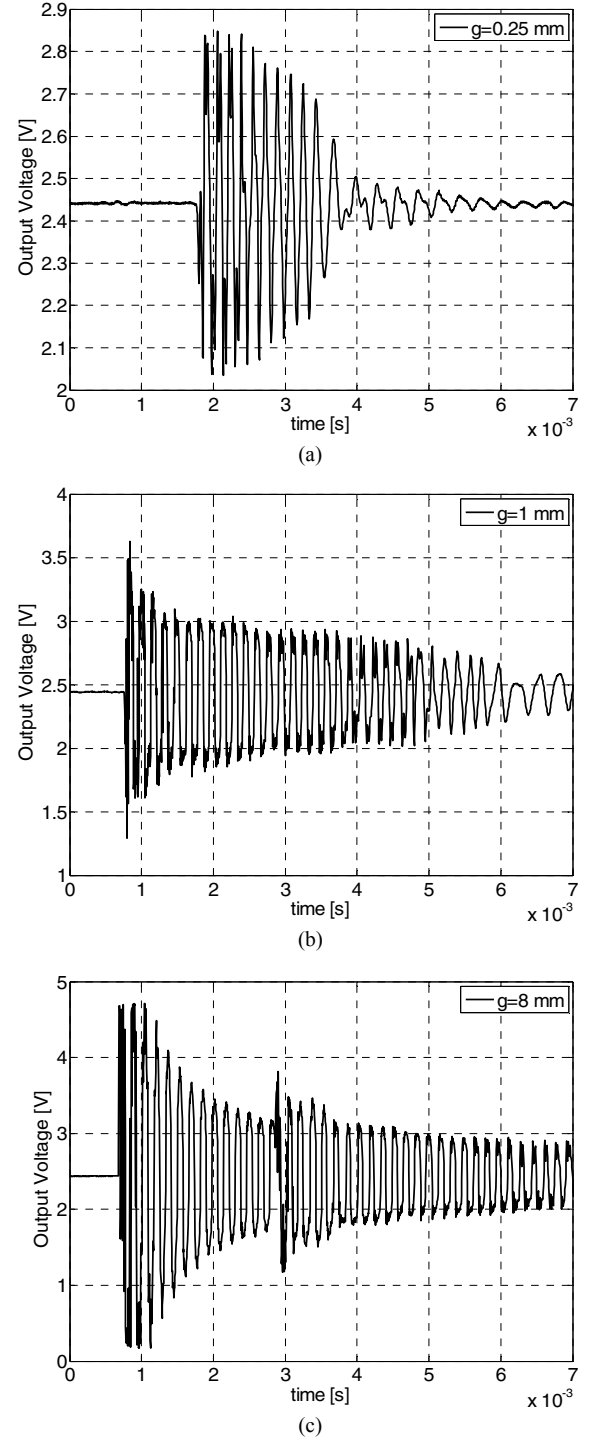


Fig. 5. The piezoelectric transducer output voltage signal due to the impact of a single ash grain for the three considered granulometries: (a) 0.25 mm, (b) 1 mm and (c) 8 mm, respectively.

shown in Fig. 8 where the curves of the Sensitivity and Specificity as the threshold value is varied for the case of discrimination between the 0.25 mm sized ash grains and the 1 mm sized grains are shown. Nevertheless, there are other analytical solutions for the choice of the optimal discrimination threshold. Three of these are presented in the following subsections.



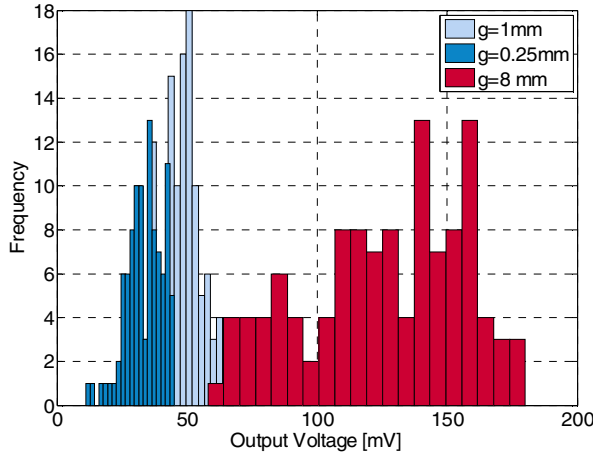
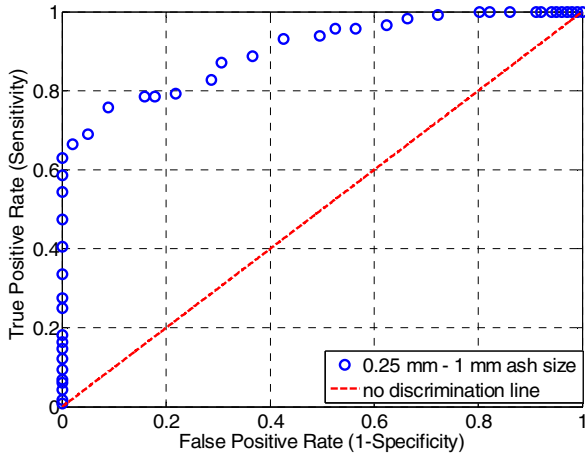
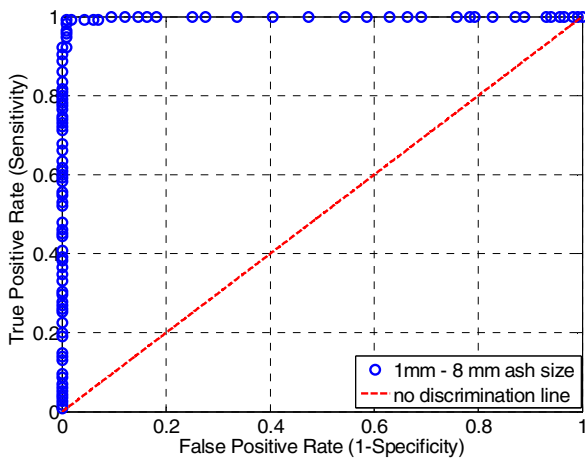


Fig. 6. Distributions of observed voltage peak amplitudes, at the output of the conditioning electronics of the piezoelectric transducer, for the three granulometries investigated.



(a)



(b)

Fig. 7. ROC curves for the volcanic ash granulometries classification. (a) Curve for the discrimination between the 0.25 mm sized ash grains and the 1 mm grains; (b) curve for the discrimination between the 1 mm sized grains and 8 mm sized grains.

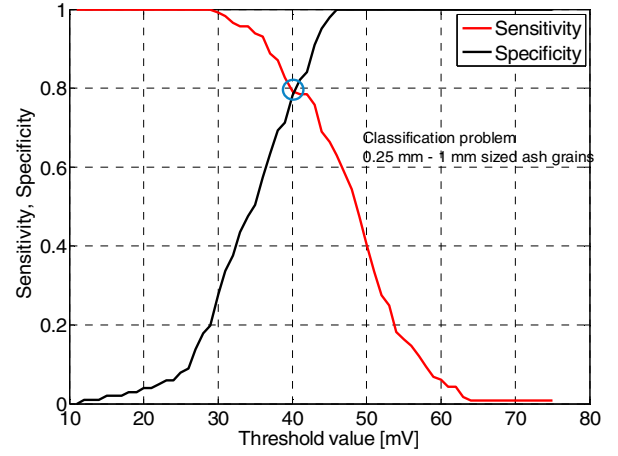


Fig. 8. Sensitivity and Specificity curves as the threshold value is varied for the case of discrimination between the 0.25 mm sized ash grains and the 1 mm sized grains.

#### A. Method 1

With reference to the example of ROC curve in Fig. 9, the first method searches for the minimum distance  $d$ , between the upper left corner having coordinates (0,1) and the points on the ROC curve:

$$\min(d = \sqrt{(1 - TPR)^2 + FPR^2}) \quad (3)$$

where TPR and FPR represent the True Positive Rate and the False Positive Rate, respectively [12, 17].

#### B. Method 2

With reference again to the ROC curve represented in Fig. 9, the second method considered here searches for the point on the curve having maximum distance  $J$  (also called Youden index) from the line of no discrimination which represents the worst case when the two classes of the problem are completely overlapped:

$$\max(TPR - FPR) \quad (4)$$

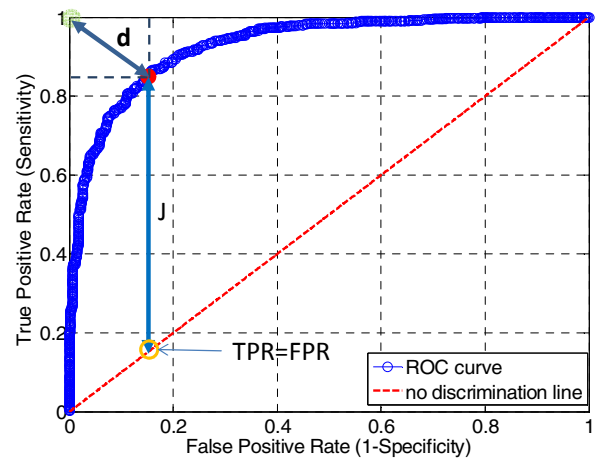


Fig. 9. Example of ROC curve and methodologies for the choice of the optimal threshold value.

### C. Method 3

Finally, the third method considered in this paper is based on the search for the threshold value providing the classifier with the maximum accuracy  $A$ , defined as:

$$A = \frac{TP + TN}{TP + TN + FP + FN} \quad (5)$$

where  $TP$ ,  $TN$ ,  $FP$  and  $FN$  represent the True Positive, True Negative, False Positive and False Negative fractions of the elements of the two classes fixed by the threshold value.

The values of the optimal threshold obtained by applying the above three methods to the two classification problems considered in this paper are reported in Table I. For the sake of comparison, the values of the thresholds obtained by considering the intersection between the Sensitivity and Specificity curves are reported in column 4 (Method 4).

As can be observed, the three above discussed methods provide the same values for the optimal discrimination threshold. A slightly lower value has been obtained by the Method 4. As already stated in [12], moving the threshold toward higher values affects the right classification of larger size ash particles (1 mm and 8 mm for the two classification problems here addressed, respectively) while it improves the correct classification of the smaller size ash particles. Since smaller particles can be transported over long distances, the effect of above choice would be the missing of warning alarms with a consequently higher risk for the safety of air transport. For the specific application addressed, a correct classification of small size particles is mandatory also at the expense of false alarms due to larger particles classified as small ash.

### VI. CONCLUSIONS

In this paper three analytical methodologies for the choice of the optimal granulometry classification thresholds by using the ROC curves theory was discussed. The three methods provided the same values for the optimal discrimination threshold. For the sake of comparison the threshold values obtained by applying an empirical methodology based on the comparison of the Sensitivity and Specificity indexes was provided. Implications due to the choice of different threshold value has been discussed. Furthermore, new experimental results obtained with a new engineered implementation of the sensor for the granulometry detection and three different granulometries (0.25 mm, 1 mm and 8 mm) was presented.

TABLE I. Optimal threshold values for the two classification problems.

	Method 1	Method 2	Method 3	Method 4
Classification 0.25 mm – 1 mm	42.99 mV	42.99 mV	42.99 mV	40.22 mV
Classification 1 mm – 8 mm	64.99 mV	64.99 mV	64.99 mV	63.98 mV

### ACKNOWLEDGMENT

This work has been developed under the SECESTA project of the POR FESR Sicilia 2007-2013, (CUP: G53F11000040004).

In particular authors wish to thanks Dr. M. Coltelli of the INGV, Catania and Eng. Mario Marino of the Ergotronica srl.

### REFERENCES

- [1] Volcanic Ash Safety in Air Traffic Management - A White Paper, European Safety Programme for ATM 2010-2014 (ESP+), June 2011 - Edition 1.0.
- [2] M. Guffanti, G. C. Mayberry, T. J. Casadevall, R. Wunderman, "Volcanic hazards to airports", *Natural Hazards*, v. 51, p. 287-302, 2009, doi:10.1007/s11069-008-9254-2.
- [3] S. Scollo, M. Prestifilippo, G. Spata, M. D'Agostino, M. Coltelli, "Monitoring and forecasting Etna volcanic plumes", *Nat. Hazards Earth Syst. Sci.* 9 (2009) 1573–1585, doi:10.5194/nhess-9-1573-2009.
- [4] G. Werner-Allen, J. Johnson, M. Ruiz, J. Lees, M. Welsh, "Monitoring Volcanic Eruptions with a Wireless Sensor Network", *Proc. of the IEEE Second European Workshop on Wireless Sensor Networks*, pp. 108-120, 2005.
- [5] P. W. Webley, K. Dean, J. E. Bailey, J. Dehn, R. Peterson, "Automated forecasting of volcanic ash dispersion utilizing Virtual Globes", *Nat. Hazards* (2009) 51:345-361, doi: 10.1007/s11069-008-9246-2.
- [6] F. Marchese, R. Corrado, N. Genzano, G. Mazzeo, R. Paciello, N. Pergola, V. Tramutoli, "Assessment of the Robust Satellite Technique (RST) for volcanic ash plume identification and tracking", *Use of Remote Sensing Techniques for Monitoring Volcanoes and Seismogenic Areas, USReST 2008. Second Workshop on*, pp. 1-5, 2008.
- [7] F. S. Marzano, E. Picciotti, G. Vulpiani, M. Montopoli, "Synthetic Signatures of Volcanic Ash Cloud Particles From X-Band Dual-Polarization Radar", *Geoscience and Remote Sensing, IEEE Trans. on*, Vol. 50, N. 1, pp. 193 – 211, 2012.
- [8] S. Corradini, C. Tirelli, G. Gangale, S. Pugnaghi, E. Carboni, "Theoretical Study on Volcanic Plume SO<sub>2</sub> and Ash Retrievals Using Ground TIR Camera: Sensitivity Analysis and Retrieval Procedure Developments, *Geoscience and Remote Sensing*", *IEEE Transactions on* vol. 48, no. 3, part 2, pp. 1619-1628, 2010, doi: 10.1109/TGRS.2009.2032242
- [9] F. S. Marzano, S. Barbieri, G. Vulpiani, W. I. Rose, "Volcanic ash cloud retrieval by ground-based microwave weather radar", *IEEE Trans Geosci. Remote Sens.* 44:3235–3246, 2006.
- [10] SECESTA project, 4.1.1.1 - POR FESR Sicilia 2007-2013, (CUP: G53F11000040004), <http://secesta.pmftraining.eu>.
- [11] B. Andò, S. Baglio, V. Marletta, "A Smart Multisensor System for the Ash Fall-Out Monitoring", *Procedia Engineering*, Volume 47, pp. 766-769, Elsevier, *Proc. of the XXVI European Conference on Solid-State Transducers EUROSENSOR 2012*, Kraków, Poland, September 9-12, 2012.
- [12] B. Andò, S. Baglio, V. Marletta, S. Medico, A Smart Multisensor System for Ash Fall-Out Monitoring, *Sensors and Actuators A: Physical*, Vol. 194, pp. 52-61, 2013.
- [13] B. Andò, S. Baglio, V. Marletta, Selective Measurement of Volcanic Ash Flow-rate, *Proceedings of the IEEE International Conference on Instrumentation and Measurement I2MTC 2013*, pp- 1367 – 1371, May 6-9, 2013, Minneapolis, MN, USA, DOI: 10.1109/I2MTC.2013.6555637.
- [14] B. Andò, S. Baglio, V. Marletta, Selective Measurement of Volcanic Ash Flow-rate, *IEEE Transactions on Instrumentation and Measurement*, vol. 63, n. 5, pp. 1356-1363, 2014.
- [15] B. Andò, S. Baglio, N. Pitrone, C. Trigona, A. R. Bulsara, V. In, M. Coltelli, S. Scollo, "A novel measurement strategy for volcanic ash fallout estimation based on RTD Fluxgate magnetometers", *Instrumentation and Measurement Technology Conference Proceedings. IMTC 2008. IEEE*, pp. 1904-1907, 2008.
- [16] B. Andò, M. Coltelli, M. Prestifilippo, S. Scollo, A lab-scale experiment to measure terminal velocity of volcanic ash, *IEEE Trans. Instrum. Meas.* 60(4) (2011) 1340–1347.
- [17] T. Fawcett, An introduction to ROC analysis, *Pattern Recognition Letters* 27 (2006) 861–874.